Available online at www.sciencedirect.com
SCIENCE DIRECT
Polymer 46 (2005) 8169–8177
polymer
www.elsevier.com/locate/polymer

Evaluation of imbedded fiber retraction phenomenological models for determining interfacial tension between molten polymers

Guillermo Palmer, Nicole R. Demarquette*

Materials Engineering Department, University of São Paulo, Av. Prof Melo Moraes 2463, 05508-900 São Paulo, Brazil

Received 9 March 2005; accepted 14 June 2005
Available online 18 July 2005

Abstract

In this work, the interfacial tension for several polymer pairs, namely polypropylene/polystyrene (PP/PS), PP/polycarbonate (PC), PP/polyamide 6 (PA-6) and low density polyethylene (LDPE) and ethylene vinyl alcohol copolymer (EVOH) was evaluated as a function of temperature using the imbedded fiber retraction method (IFR). Two phenomenological models were used and compared to infer the interfacial tension from the evolution of the imbedded fiber back into a sphere: [Carriere CJ, Cohen A, Arends CB. J Rheol 1989;33:681–9. [1] and Tjahjadi M, Ottino JM, Stone HA. AIChE J 1994;40:385–94. [2]]. It was shown that Carriere et al.'s model overestimates the value of interfacial tension whereas Tjahjadi et al.'s model leads to results that corroborate the ones obtained using other experimental methods. A method to further increase the accuracy of Tjahjadi et al.'s model was proposed. Using this method the interfacial tension for the different polymer pairs studied was evaluated and shown to decrease linearly with increasing temperature.

Keywords: Polymer blends; Interfacial tension; Imbedded fiber retraction method

1. Introduction

Interfacial tension in molten polymers is one of the major factors governing the morphology of binary blends and, therefore, the final physical and mechanical properties of the product [3]. Unfortunately, the experimental determination of interfacial tension in molten polymers is a difficult task owing to the high viscosity and rheological characteristics of those materials. Several experimental methods have been used to evaluate interfacial tension between molten polymers. A thorough review of the different methods for direct measurement of interfacial tension between molten polymers can be found in [4].

The imbedded fiber retraction (IFR) method is a dynamic technique that has been used to measure the interfacial tension between molten polymers [1,2,5–10]. The method involves the analysis of the evolution of the shape of a short fluid thread embedded in another fluid, from which interfacial tension can be inferred using two models: Carriere et al. [1] and Tjahjadi et al. [2]. Other theories [11–19] have been developed to study the retraction of an ellipsoid into a sphere but cannot be applied to model the retraction of a fiber into a sphere because of the intermediate dumbbell shape that the fiber adopts during the retraction process. In this work, Carriere et al. and Tjahjadi et al.'s phenomenological models were evaluated as tools to infer interfacial tension between molten polymers from the retraction of a fiber.

The first part of the paper summarizes Carriere et al. and Tjahjadi et al.'s models. In the second part, the experimental procedures used to study the fiber retraction process are described. Finally, the experimental results obtained for polypropylene/polystyrene, polypropylene/polycarbonate, polypropylene/polyamide-6 and low density polyethylene/ethylene vinyl alcohol copolymer polymer pairs are presented, discussed and the values of interfacial tension obtained using both theories are compared to the literature.

* Corresponding author. Tel.: +55 113 091 5693; fax: +55 113 091 5243.
E-mail address: nick@usp.br (N.R. Demarquette).

0032-3861/$ - see front matter © 2005 Elsevier Ltd. All rights reserved.
doi:10.1016/j.polymer.2005.06.047

2. Theories

2.1. Imbedded fiber retraction (IFR) method

The IFR method involves the analysis of the change of shape of a short fiber of fluid embedded in a matrix of another fluid. Fibers of molten polymers with an aspect ratio lower than a critical value that depends on the ratio of viscosity of the fiber and of the matrix [2] will retract into a sphere as shown in Fig. 1. From the study of the evolution of the fiber and the knowledge of the zero shear viscosity of the polymers involved, it is possible to infer the interfacial tension between those two polymers. Two phenomenological models have been developed to infer interfacial tension between molten polymers from the study of the retraction of the fiber: Carriere et al. [1] and Tjahjadi et al. [2]. They are reviewed briefly below.

2.2. Carriere et al.'s model

In this model, Carriere et al. showed that the evolution of a fiber into a sphere can be described by (Eq. (1)):

$$f\left(\frac{R_{if}}{R_e}\right) - f\left(\frac{R_{0if}}{R_e}\right) = \frac{1}{t_{c1}}t \tag{1}$$

with

$$f(x) = 3\ln\left\{\frac{(1+x+x^2)^{1/2}}{1-x}\right\} + 3^{3/2}\tan^{-1}\left(\frac{3^{1/2}x}{2+x}\right) - x - 8x^{-2} \tag{2}$$

and

$$t_{c1} = \frac{\eta_{ef}R_e}{\gamma} \tag{3}$$

where R_{0if}, R_{if} and R_e are, respectively, the initial radius of the fiber, the effective radius of the retracting fiber and the radius of a sphere having the same volume as the fiber as illustrated in Fig. 1, t is the retraction time, t_{c1} is a characteristic time for retraction from Carriere et al.'s model, γ is the interfacial tension between the two polymers involved in the experiment and η_{ef} is an effective viscosity which is a function of the viscosities of both polymers.

The effective radius of the retracting fiber was defined by Cohen and Carriere [7] for a uniform cylinder with hemispherical ends and $2L_{if}/R_e > 2$ by (Eq. (4)):

$$R_{if} = L_{if}(1 - \cos\varphi + \sqrt{3}\sin\varphi) \tag{4}$$

with

$$\varphi = \frac{1}{3}\tan^{-1}\left\{\frac{4\left[\left(\frac{2L_{if}}{R_e}\right)^3 - 4\right]^{1/2}}{\left(\frac{2L_{if}}{R_e}\right)^3 - 8}\right\} \tag{5}$$

The plot of Eq. (1) as a function of time results in a straight line with a slope proportional to the interfacial tension between the two polymers. Therefore, once the geometrical parameters of the evolving fiber are measured, and if the rheological characteristics of the polymers are known, the interfacial tension can be inferred. More details about the model can be found in Refs. [1,5–7,10]. The

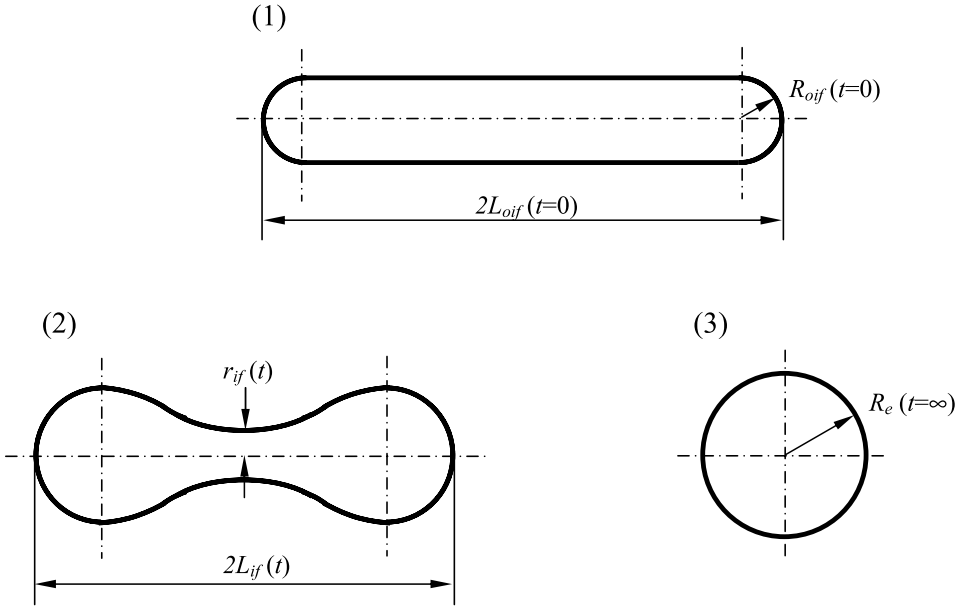

Fig. 1. Illustration of imbedded fiber during the retraction process.

Carriere et al.'s model requires the determination of the effective viscosity η_{ef} which was determined, empirically, by Carriere et al. for PS/PMMA as (Eq. (6)):

$$\eta_{ef} = \eta_{0m}\frac{1.7\lambda + 1}{2.7} \tag{6}$$

with

$$\lambda = \frac{\eta_{0f}}{\eta_{0m}} \tag{7}$$

where λ is the viscosity ratio of the fiber to the matrix, η_{0m} and η_{0f} are, respectively, the zero shear viscosity of the matrix and the fiber.

More details about the theory can be found in the original work of Carriere et al. [1].

2.3. Tjahjadi et al.'s model

Tjahjadi et al. [2] presented another model to determine the interfacial tension between two Newtonian fluids from short fiber retraction. The theory used curve—fitted polynomials to describe the length of the retracting fiber, calculated from numerically generated results of the transient shapes using boundary integral techniques. The decrease in length of the fiber as a function of the viscosity ratio, λ, and dimensionless computational time, τ, is given by (Eq. (8)):

$$\frac{L(\tau)}{R_e} = \sum_{n=0}^{4} k_n(\lambda)\tau^n \tag{8}$$

where R_e is the radius of a sphere having the same volume as the fiber as illustrated in Fig. 1, the five coefficients k_0-k_4 for different viscosity ratios and initial aspect ratios, AR, can be found in the article of Tjahjadi et al. [2], η_{0m} and η_{0f} are, respectively, the zero shear viscosity of the matrix and the fiber, $L(\tau)$ is the half length of the fiber at a time τ, and τ a dimensionless computational time defined by (Eq. (9)):

$$\tau = \frac{t}{t_{c2}} \tag{9}$$

where t is the real time of the experiment and t_{c2} is a characteristic time for the interfacial tension driven motions in the experiment given by (Eq. (10)):

$$t_{c2} = \frac{R_{0if}\eta_{0m}}{\gamma} \tag{10}$$

where R_{0if} is the initial radius of the fiber as illustrated in Fig. 1 and γ is the interfacial tension between molten polymers.

To infer the interfacial tension from the retraction of a fiber using Tjahjadi et al.'s model, two images of the fiber while retracting at two different times t_1 and t_2 (with $\Delta t_{exp} = t_2 - t_1$) are analysed and the corresponding fiber half lengths for both images are measured. Independently, $L(\tau)/R_e$ is plotted using Eq. (8) and the coefficients k_n for the appropriate viscosity ratio. Using the curve plotted and the experimental values of $L(t)/R_e$ for both images (Tjahjadi et al. [2] recommend that $L(t)/R_e > 1.5$), it is possible to determine $\Delta\tau_{theo}$ which corresponds to the theoretical time interval between both images. $\Delta\tau_{theo}$ is then compared to Δt_{exp} and the interfacial tension can be inferred using Eqs. (9) and (10). More details about the theory can be found in the original work of Tjahjadi et al. [2].

In this work, both phenomenological models, Carriere et al. and Tjahjadi et al. were tested and evaluated to infer interfacial tension from the study of the dynamic of fiber retraction.

3. Materials

Table 1 shows the characteristics of the materials used in this study. One polypropylene (PP) was used in this work to evaluate the interfacial tension between PP/Polystyrene (PS), PP/Polycarbonate (PC) and PP/Polyamide-6 (PA-6). The interfacial tension also was determined for low density polyethylene (LDPE) and Ethylene vinyl alcohol copolymer (EVOH) polymer pair.

3.1. Sample preparation

The fiber used in this work, to evaluate the interfacial tension between PP/PS and PP/PC were prepared from PP to satisfy that the viscosity ratio, λ, be smaller than one and the softening temperature of the matrix be smaller than the softening temperature of the fiber simultaneously. It has been shown in the literature [20] that if the viscosity ratio, λ, is higher than one phenomenon such as end pinching or retraction could occur and if the softening temperature of the matrix is higher than the softening temperature of the fiber air bubbles could be appear between the fiber and matrix during the imbedding process. To satisfy these two conditions, the fibers used to evaluate the interfacial tension for PP/PA-6 and EVOH/LDPE polymer pairs were prepared from PA-6 and EVOH, respectively.

The fibers were obtained by melt spinning of molten pellets using a hot plate. The fibers diameters varied from 0.05 to 0.15 mm. The fibers were annealed during 24 h (72 h for PA-6) under vacuum (below 10 mmHg) between 10 and 15 °C below the respective softening temperature to avoid residual stresses. The fibers used were cut into pieces of 1–2 mm prior to annealing. The aspect ratio $AR = L_{0if}/R_{0if}$ (where L_{0if} and R_{0if} are the half length and radius of the fiber for $t = 0$ s, respectively) were chosen so that it would be lower than a critical value that depends on the viscosity ratio, λ [2]. The films (matrix) used in the experiments were obtained by compression molding. The matrix samples were molded at a temperature of 180 °C with holding time of 10 min at 180 MPa. The thickness of the films (matrix) varied from 0.25 to 1 mm to minimize eventual problems with air bubbles and to promote a melting process fast

Table 1
Materials used in this work

Polymer	MFI (g/10 min)	η_0 (Pa s)			T_g (°C)	T_m (°C)	Supplier	Specification
		200 °C	220 °C	240 °C				
PP	16.5	1800	1600	970	−5	163	Polibrasil	TS6100
OS	2.5	9900	5300	2600	103	–	BASF	145H
PC	20	43,400	11,300	3500	151	–	Bayer	2458
PA-6	25*	–	–	240	60	235	Massa Ferro	Mazmid B260
EVOH	–	3500	2100	1500	49	184	Aldrich Chemical	41.409-3
LDPE	1.5	70,600	38,600	26,400	−130	114	Aldrich Chemical	42.802-7

MFI is the melt flow index; η_0 is the zero shear viscosity.

enough to avoid fiber distortion to start before complete melting of the films.

3.2. Zero shear viscosity measurements

The values of zero shear viscosity necessary to determine the interfacial tension by IFR method were evaluated using a stress-controlled rheometer (model SR-5000 from Rheometric Scientific®). The rheological tests were carried out under a dry nitrogen atmosphere using 25 mm diameter and 1.5 mm thickness samples, obtained by compression molding at temperature of 180 °C (or 240 °C for PA-6) with holding time of 10 min at 180 MPa. Frequency sweep experiments were performed over a frequency range of 0.01–300 rad/s.

The zero shear viscosity (η_0) of the polymers, necessary to evaluate interfacial tension using both phenomenological models, were inferred fitting Carreau Model [21,22] to plots of the complex viscosity (η^*) against frequency using Rheometrics Orchestrator software. The values for the zero shear viscosity of the each polymer are summarized in Table 1.

Polyamides are thermally unstable at high temperatures and the evaluation of their zero shear viscosity is difficult because it requires long exposure times at high temperature In this work, the zero shear viscosity of PA-6 at a temperature of 240 °C was determined using rheological measurements that were performed using seven different sequences of frequencies. Using this procedure, it was possible to reduce the exposure time of the polymer at high temperature and avoid thermal degradation.

3.3. Interfacial tension experimental procedure

The experiments were carried out placing the fibers between two films of the matrix. The 'sandwiches' formed were placed between two glass sheets and heated in a hot stage (Mettler FP-90). The temperature was raised at a rate of 20 °C/s to 10 or 15 °C above the respective softening temperature of the polymers forming the matrix. The system was maintained at this temperature to allow all the air bubbles to escape. After the melt front had closed around the fibers, the 'sandwiches' were annealed during 10 h under vacuum at 10 °C above the softening temperature of matrix polymers to eliminate residual stresses. Then, the 'sandwiches' were placed again in the hot stage and the temperature was raised to the temperature at which the experiment was performed (200, 220 or 240 °C). The visualization of the retracting process was made using an optical microscope at a magnification of 50× or 100× depending on the radius of the fiber. Photos of the retraction process were taken using a CCD camera. The images were then analyzed using a commercial digital image analysis software package. The fibers dimensions were measured as a function of time and used to calculate the interfacial tension.

4. Results and discussion

Fig. 2 shows the evolution of fibers of PP imbedded in PC at a temperature of 240 °C, as a function of time for three different values of initial aspect ratio. It can be seen that for moderately extended fiber, when the aspect ratio is smaller than the one that can be found using Tjahjadi et al. [2] criteria for $\lambda = 0.227$, i.e. $AR < AR_{crit}(0.277) = 12/16$, the fiber retracts back towards a spherical shape without breakup (Fig. 2(a) and (b)). As the aspect ratio of the initial fiber tends toward $AR_{crit}(\lambda)$, a more pronounced dumbbell intermediate shape is observed before reaching the final spherical shape. When $AR > AR_{crit}(0.277) = 12/16$ [2], the fiber evolves into a dumbbell shape with two bulbous ends and break-up occurs (Fig. 2(c)).

Fig. 3 presents the dimensions $L_{if}(t)/R_{ec}$ and $r_{if}(t)/R_{ec}$ for fibers of PP imbedded in PC at a temperature of 240 °C for different aspect ratios ($AR = L_{0if}/R_{0if}$), where, $L_{if}(t)$ and $r_{if}(t)$ are the half length and the radius of the fiber at a time t as shown in Fig. 1 while R_{ec} is the radius of the equivalent sphere calculated from fiber volume at a time $t = 0$. It can be seen that at the beginning of the retraction process ($t < 80$ s) the values of the shape function, $r_{if}(t)/R_{ec}$, keeps constant and is independent of the fiber aspect ratio (AR) except for

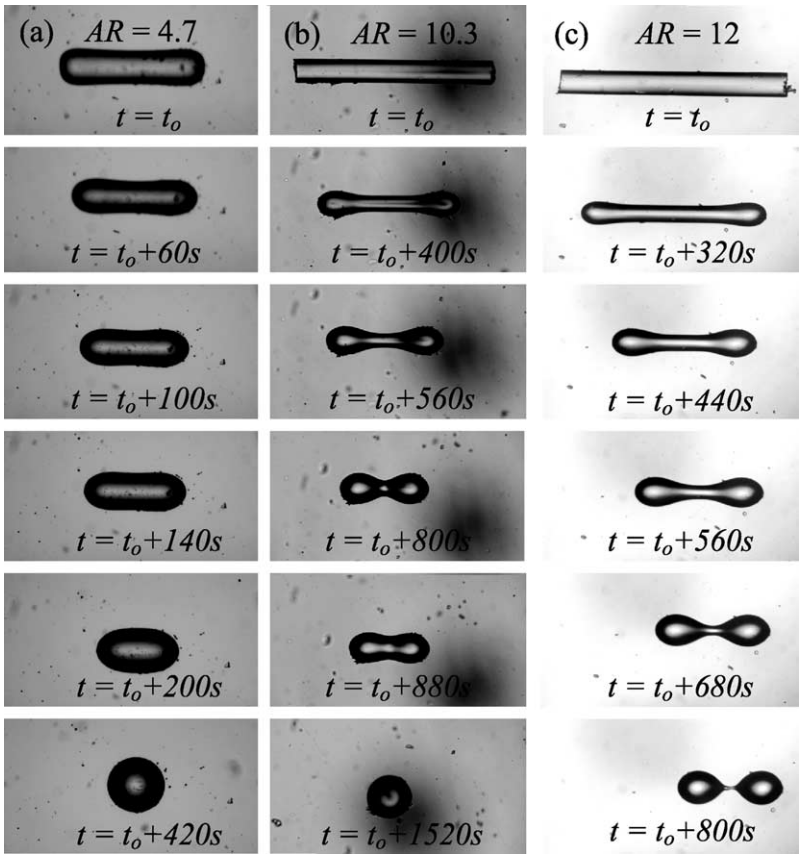

Fig. 2. Evolution of fibers of PP imbedded in PC with different aspect ratio AR, (a) AR = 4.7; (b) AR = 10.3; (c) AR = 12. The viscosity ratio is 0.277.

AR = 12. For times greater than 80 s three types of behavior that correspond to the images of Fig. 2 can be observed:

(a) For AR < 8: Short fibers, the shape function decreases rather slowly, reaches a minimum value and increases to one, that corresponds to the end of the retracting process.

(b) For $8 \leq AR < 12$: Medium size fibers, the shape

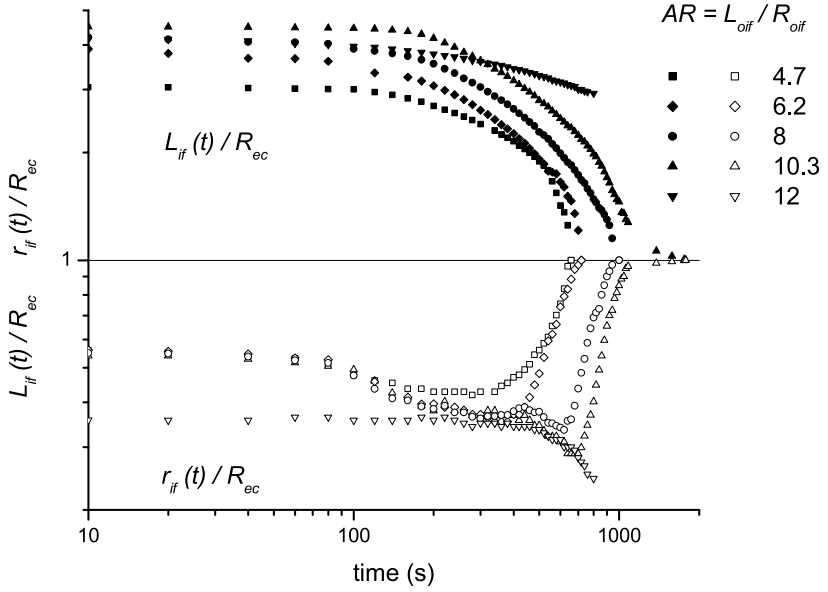

Fig. 3. Time dependence of $L_{if}(t)/R_{ec}$ and $r_{if}(t)/R_{ec}$ for fibers of PP imbedded a matrix of PC at a temperature of 240 °C for different aspect ratios (AR). ($L_{if}(t)$, half length of the fiber at a time t; $r_{if}(t)$, radius of the fiber at a time t; L_{0if}, half length of the fiber at $t=0$; r_{0if}, radius of the fiber at $t=0$ and R_{ec}, radius of the equivalent sphere calculated from fiber volume at $t=0$).

function decreases rather slowly, stabilizes for some time, then decreases quickly, reaching a minimum value, and finally increases to one.

(c) For AR ≥ 12, the shape function, $r_{if}(t)/R_{ec}$, lower than for the other AR, keeps constant for a larger amount of time (500 s), decreases until the fiber breaks into two spheres.

This division in three types of behavior was observed for all the polymer pairs studied in this work. The values of critical aspect ratios, corresponding to the largest aspect ratio for the fiber to not undergo breakup, found experimentally for the different viscosity ratios of the polymer pairs studied in this work are reported in Table 2. They were found to corroborate the values reported by Tjahjadi et al. [2] obtained via boundary integral techniques.

The evolution of the geometrical dimensions of the fibers was used to evaluate the interfacial tension for the polymer pairs studied using Carriere et al.'s and Tjahjadi et al.'s models. Fig. 4 shows the imbedded fiber retraction function, $f(R_{if}/R_e)$ vs time, using Carriere et al.'s model for a fiber of PP imbedded in PC at 240 °C. It can be seen that within experimental error, $f(R_{if}/R_e)$ as a function of time is a straight line from which the interfacial tension can be inferred using Eq. (3). Table 3 presents the coefficients of linear square regression of the data obtained by fitting the $f(R_{if}/R_e)$ as a function of time. Two time ranges were considered: (a) a time range corresponding to the whole experiment 100 s $< t <$ 1000 s. (b) A time range corresponding to times near the minimum value of the shape function (620 s $< t <$ 820 s). It can be seen from the values reported in Table 3, that a much better fitting is obtained when only the data corresponding to the shorter time range are considered. It can also be seen from the values reported in Table 3 that the fitting corresponding to the shorter time range leads to smaller values of interfacial tension. Similar behavior was obtained for all the polymer pairs studied in this work. Table 4 presents the values of interfacial tension found using Carriere et al.'s model, taking into considerations the values of the $f(R_{if}/R_e)$ as a function of time corresponding to the time range near the minimum value of $r_{if}(t)/R_{ec}$. The values are compared to the ones reported in other works and the ones obtained by harmonic and geometric means. It can be seen that the values obtained using Carriere et al.'s model are much larger than the ones reported in the literature for the same polymer pairs even though only the data corresponding to time range near the minimum value of $r_{if}(t)/R_{ec}$ were considered. This discrepancy could be due to the use of Eq. (6) to evaluate the effective viscosity of the polymer pairs studied here. Eq. (6) was determined empirically by Carriere et al. for polystyrene (PS)/poly(methyl methacrylate) (PMMA) polymer pair and may not be adequate for other polymer pairs.

Table 3
Linear regression coefficients of $f(R_{if}/R_e) = a(t) - b$

Time range (s)	$a = \gamma/(R_e\eta_{ef})$	B	r^2
100–1000	0.044	49	0.983
620–820	0.034	42	0.996

Table 5 shows the values of interfacial tension between PP and PC at 240 °C obtained using the analysis of Tjahjadi et al. for two different aspect ratio, L_{0if}/R_{0if}, 10.3 and 4.7, respectively. The time reported in the horizontal line corresponds to t_1: Time at which the first image for the analysis is taken, and the time reported in the vertical line corresponds to t_2: Time at which the second image for the analysis is taken. It can be seen that the values of interfacial tension determined using two images corresponding to retraction times far from the minimum of the curves shown in Fig. 3 are higher than the ones obtained using two images corresponding to retraction times near the minimum value of shape function, $r_{if}(t)/R_{ec}$. Similar behavior was observed for all experiments.

The values of interfacial tension obtained using Tjahjadi et al.'s analysis when taking into considerations measurements corresponding to the minimum values of shape function, $r_{if}(t)/R_{ec}$ are presented in Table 4. It can be seen that the values obtained corroborate, within experimental error, the ones obtained using other methods. The results presented in Tables 4 and 5 indicate that in order to entrance the accuracy of Tjahjadi et al.'s method data corresponding to the minimum of $r_{if}(t)/R_{ec}$ should be taken into account.

Table 6 shows the linear regression coefficients corresponding of the interfacial tension values obtained using Tjahjadi et al.'s model for PP/PS; PP/PC and LDPE/EVOH polymer pairs. It can be seen that for the three polymer pairs studied in this work the interfacial tension decreases linearly with increasing temperature, which is expected thermodynamically. The order of magnitude of $-\partial\gamma/\partial T$ found in this work corroborate the ones found in the literature [20,23–25].

5. Conclusions

The interfacial tension between polypropylene (PP) and polystyrene (PS), PP and polycarbonate (PC), PP and polyamide 6 (PA-6) and low density polyethylene (LDPE)

Table 2
Critical aspect ratio, AR_{crit}, as a function of viscosity ratio, λ

$\lambda(\eta_{0f}/\eta_{0m})$	0.04–0.06	0.11–0.18	0.19	0.24–0.27	0.31	0.37	0.57
$AR_{crit}(\lambda)(\pm 0.5)$	10	11	11.5	12	19	21	24

η_{0f} and η_{0m} are zero shear viscosity of the fiber and matrix, respectively.

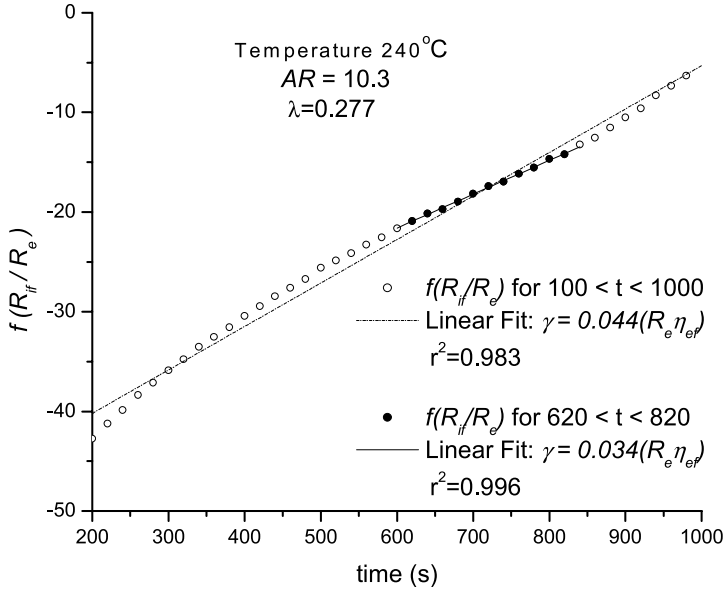

Fig. 4. Representative imbedded fiber retraction data for a fiber of PP imbedded in PC from Carriere et al.'s model at 240 °C. The interfacial tension is proportional to the slope of line fit through the experimental data.

and ethylene vinyl alcohol copolymer (EVOH) has been evaluated using the imbedded fiber retraction method. Two phenomenological models were used and compared to evaluate interfacial tension from the study of the dynamic of the evolution of the fiber back into a sphere: Carriere et al. [1] and Tjahjadi et al. [2]. The following conclusions could be drawn from the study.

(1) Three types of behavior can be observed when studying the retraction of an imbedded fiber depending on the initial aspect ratio (AR) of the fiber. If AR is larger than a critical value (AR_{crit}), that depends on the viscosity ratio of the two polymers involved in the interfacial tension measurement, the fiber evolves into a dumbbell shape with two bulbous ends and break-up occurs. If the AR is slightly smaller than AR_{crit} the fiber evolves into a dumbbell shape and retracts into one sphere. As AR is decreased no dumbbell shape is observed.

(2) The three types of behavior described above can be identified by plotting the function $r_{if}(t)/R_{ec}$ (where $r_{if}(t)$ and R_{ec} are the radius of the fiber at a time t and of the equivalent sphere calculated from fiber volume at a time $t=0$, respectively) as a function of time. At the beginning of the retraction phenomenon $r_{if}(t)/R_{ec}$ keeps constant and is independent of the AR provided $AR < AR_{crit}$. If $AR > AR_{crit}$ this value is much smaller. This criterion allows the choice of fiber dimensions to perform an imbedded fiber experiment. If AR is much smaller than AR_{crit} and no dumbbell shape is observed, $r_{if}(t)/R_{ec}$ decreases after the initial time reaches a

Table 4
Interfacial tension in mN/m for the different polymer pairs studied in this work

Materials	T (°C)	Imbedded fiber retraction		Breaking Thread Palmer and Demarquette 2003 (±0.4)	Pendant Drop Arashiro and Demarquette 1999 (±0.25)	Mean equation	
		Carriere et al. (±0.9)	Tjahjadi et al. (±0.4)			H	G
PP/OS	200	11.2	5	5.8	6.5	5.02	4.8
	220	9.8	4.7	5.1	5.1	4.9	4.6
	240	8.5	4.5	4.5	4.83	4.5	4.4
PP/PC	200	18.3	12	12.6		12.1	11.8
	220	14	10.2	10.6		10.1	9.8
	240	11.3	8	8.5		8	7.7
PP/PA-6	240	16.7	12.2				
LDPE/EVOH	200	47	27.9				
	220	46	26.4				
	240	44.6	24.5				

Table 5
Interfacial tension calculated using Tjahjadi et al.'s model between PP/PC at 240 °C, $\lambda = 0.277$

Interfacial tension (mN/m)													
$L_{0if}/R_{0if} = 10.3$							$L_{0if}/R_{0if} = 4.7$						
Time (s)	200	400	500	600	700	800	Time (s)	180	220	260	300	380	500
900	8.6	7.8	7.5	7.5	7.8	8.4	540	7.7	7.6	7.6	7.5	7.9	8.7
860	8.5	7.6	7.3	7.1	7.2	7.2	520	7.6	7.4	7.4	7.3	7.6	7.8
820	8.5	7.6	7.1	6.9	6.8	5.2	500	7.6	7.4	7.4	7.3	7.6	
780	8.6	7.7	7.2	6.9	6.8		480	7.5	7.3	7.3	7.1	7.3	
740	8.7	7.7	7.2	6.8	6.4		460	7.5	7.3	7.3	7.1	7.3	
700	8.9	7.9	7.3	7			440	7.5	7.3	7.3	7.1	7.3	
660	9	8	7.3	6.6			420	7.6	7.3	7.3	7.1	7.5	
620	9.3	8.3	7.7	7.4			400	7.5	7.2	7.2	6.8	6.8	
580	9.4	8.3	7.5				380	7.6	7.3	7.2	6.9		
540	9.6	8.5	7.1				360	7.7	7.3	7.3	6.9		
500	9.9	9					340	7.7	7.3	7.2	6.5		
460	10	8.8					300	8. 1	7.6	7.3			
420	10.2	9.1					280	8	7.4	7.4			
380	10.4						260	8.1	7.3				
340	10.8						240	8.4	7.3				
300	11.1						220	8.9					
260	11.5						200	9.4					

L_{0if} and R_{0if} are the half length and the radius of the fiber at $t = 0$, respectively.

Table 6
Linear regression coefficients of $\gamma = a - bT$ ($200 \leq T \leq 240$)

Polymer pair	a	B	r^2
PP/PS	7.515	0.0128	0.99
PP/PC	33.035	0.1052	0.997
PELD/EVOH	45.032	0.0852	0.996

minimum and then increases to one. If a dumbbell shape is observed, $r_{if}(t)/R_{ec}$ decreases after the initial time levels off, reaching a plateau. After that it reaches a second minimum before increasing to one.

(3) The accuracy of the imbedded fiber retraction (IFR) method was enhanced if only the fibers that correspond to the plateau region are considered in the calculation. This was observed when using both models Carriere et al. [1] and Tjahjadi et al. [2].
(4) Carriere et al.'s theory overestimates the values of interfacial tension for the polymer pairs studied here. This was attributed to the use of an empirical expression to determine the effective viscosity of the polymer pair, in the theory.
(5) The values of interfacial tension obtained by Tjahjadi et al.'s theory corroborate the ones obtained with other experimental method showing the accuracy of the method.
(6) For all the polymer pairs studied (PP/PS, PP/PC, PP/PA-6 and LDPE/EVOH) the interfacial tension decreases linearly with increasing temperature.

Acknowledgements

The authors would like to thank the Polibrasil SA, BASF, Uniflon and Bayer for supplying the materials and FAPESP Brazilian Funding Agency for Financial Support.

References

[1] Carriere CJ, Cohen A, Arends CB. J Rheol 1989;33:681–9.
[2] Tjahjadi M, Ottino JM, Stone HA. AIChE J 1994;40:385–94.
[3] Utracki LA. Encyclopaedic dictionary of commercial polymer blends. Toronto, Canada: Chemtec Publishing; 1996.
[4] Demarquette NR. Mater Rev 2003;48(4):247–9.
[5] Carriere CJ, Biresaw G, Sammler RL. Rheol Acta 2000;39:476–82.
[6] Carriere CJ, Cohen A. J Rheol 1991;35:205–12.
[7] Cohen A, Carriere CJ. Rheol Acta 1989;28:223–32.
[8] Ellingson PC, Strand DA, Cohen A, Sammler RL, Carriere CJ. Macromolecules 1994;27:1643–7.
[9] Sammler RL, Dion RP, Carriere CJ, Cohen A. Rheol Acta 1992;31:554–64.
[10] Biresaw G, Carriere CJ, Sammler RL. Rheol Acta 2003;42:142–7.
[11] Luciani A, Champagne MF, Utracki LA. J Polym Sci, Phys Ed 1997;35:1393–403.
[12] Sigillo I, Santo L, Gudi S, Grizzuti N. Polym Eng Sci 1997;37(9):1540–9.
[13] Yamane H, Takahashi M, Hayashi R, Okamoto K. J Rheol 1998;42:567–80.
[14] Maffettone PL, Minale M. J Non-Newtonian Fluid Mech 1998;78:227–41.
[15] Mo H, Zhou C, Yu W. J Non-Newtonian Fluid Mech 2000;91:221–32.
[16] Wetzel ED, Tucker CL. J Fluid Mech 2001;426:199–228.
[17] Son Y, Migler KB. Polymer 2002;43:3001–6.
[18] Wu Y, Zinchenko AZ, Davis RH. J Non-Newtonian Fluid Mech 2002;102:281–98.
[19] Wu Y, Zinchenko AZ, Davis RH. Ind Eng Chem Res 2002;41:6270–8.
[20] Palmer G, Demarquette NR. Polymer 2003;44:3045–52.
[21] Bird RB, Armstrong RC, Hassager O. Dynamics of polymeric liquids 2nd ed vol. 1. New York: Wiley; 1987. p. 169–75.
[22] Carreau PJ, De Kee D, Chhabra R. Rheology of polymeric systems principles and applications. New York: Carl Hanser Verlag; 1997.
[23] Everaert V, Groeninckx G, Pionteck J, Favis BD, Aerts L, Moldenaers P, et al. Polymer 2000;41:1011–25.
[24] Visscher EJ, Willemse RC. Polym Eng Sci 1999;39(7):1251–6.
[25] Arashiro EY, Demarquette NR. Mater Res 1999;1(2):1–10.